Aminoglycoside Binding to *Oxytricha nova* Telomeric DNA[†]

Nihar Ranjan, Katrine F. Andreasen, Sunil Kumar, David Hyde-Volpe, and Dev P. Arya*

Laboratories of Medicinal Chemistry, Clemson University, Clemson, South Carolina 29634, United States

Received September 17, 2010

ABSTRACT: Telomeric DNA sequences have been at the center stage of drug design for cancer treatment in recent years. The ability of these DNA structures to form four-stranded nucleic acid structures, called G-quadruplexes, has been perceived as target for inhibiting telomerase activity vital for the longevity of cancer cells. Being highly diverse in structural forms, these G-quadruplexes are subjects of detailed studies of ligand−DNA interactions of different classes, which will pave the way for logical design of more potent ligands in future. The binding of aminoglycosides was investigated with *Oxytricha nova* quadruplex forming DNA sequence (GGGGTTTTGGGG)$_2$. Isothermal titration calorimetry (ITC) determined ligand to quadruplex binding ratio shows 1:1 neomycin:quadruplex binding with association constants (K_a) ∼ $10^5 \, M^{-1}$ while paromomycin was found to have a 2-fold weaker affinity than neomycin. The CD titration experiments with neomycin resulted in minimal changes in the CD signal. FID assays, performed to determine the minimum concentration required to displace half of the fluorescent probe bound, showed neomycin as the best of the all aminoglycosides studied for quadruplex binding. Initial NMR footprint suggests that ligand−DNA interactions occur in the wide groove of the quadruplex. Computational docking studies also indicate that aminoglycosides bind in the wide groove of the quadruplex.

The emergence of G-quadruplexes as potential telomerase inhibitors shows considerable promise for combating cancer (*1−4*). The biological relevance of such structures lies in the propensity of many telomeric and promoter sequences to form G-quadruplexes under physiological conditions (*5*). Increased expression of telomerase, a ribonucleoprotein, has been suggested to be one of the main reasons for the immortality of cancer cells (*6−9*). The telomerase-induced immortality to cancer cells stems from its ability to act as a reverse transcriptase, elongating curtailed single-stranded telomeric ends (*10*). However, for its activity, telomerase requires chromosomal ends to be single stranded. Therefore, ligands that are capable of keeping these ends in non-single-stranded forms, such as G-quadruplexes, are attractive for cancer treatment (*1*). While there are a plethora of duplex DNA binding ligands, the number of ligands that bind to G-quadruplexes is smaller but growing rapidly (*11*). This necessitates the search for new compounds to advance G-quadruplex-based drug design. Herein, we report the discovery of aminoglycoside (specifically neomycin and paromomycin) ligand binding to *Oxytricha nova* G-quadruplex DNA.

G-quadruplex nucleic acid structures, discovered by Davies and co-workers in 1962, use four DNA/RNA guanine bases to form a planar arrangement connected by eight Hoogsteen-paired hydrogen bonds (Figure 1A) (*12, 13*). The planar arrangement of these guanine bases gives rise to the formation of a G-tetrad, which has a central cavity stabilized by metal cations such as K^+ and Na^+ (*14*). These nucleic acid structures are broadly classified into two categories, "parallel" and "antiparallel", depending upon the orientation of strands and utilize one or more strands for their formation (Figure 1B). There are many variants of these structures which are often dictated by loops and the nature of stabilizing metal cations.

To date, several types of ligands have been reported to bind to different types of G-quadruplexes. Most of these ligands have a common feature of being planar compounds such as anthraquinones (*15*), porphyrin derivatives (*16−18*), quinacridines (*19*), anthracenediones (*20*), triarylpyridines (*21*), oxazole-containing macrocyclic compounds (*22*), cationic corrole derivatives (*23*), steroid derivatives (*24*), and berberine derivatives (*25*) to name a few. Classical duplex minor groove binders such as distamycin (*26, 27*) and Hoechst 33258 (*28*) have also been shown to interact with G-quadruplex structures with less affinity and different modes of interactions than duplex DNA. Interestingly, the majority of the ligands that bind to G-quadruplexes has been proposed to have stacking interactions between G-tetrads or simply binding at the ends (*11*). Ligands that selectively recognize G-quadruplex grooves are few even though quadruplex groove recognition is likely to provide much more quadruplex-selective ligands (*29*). The development of ligands that can possibly recognize G-quadruplex through non-stacking mechanisms is essential for complementing existing approaches for recognition of G-quadruplexes.

In recent years, numerous targets of aminoglycosides have been uncovered. This includes group I introns, the rev response element, ψ-element of HIV-1 virus, and hammerhead ribozymes (*30−32*), as well as single-stranded nucleic acids (poly(A)) (*33*). We have expanded this list to triple helical nucleic acids comprised of DNA, RNA, or hybrid structures (*34−40*) and shown that the recognition domain for aminoglycosides is not just limited to RNA targets but to structures that adopt A-form (*41−44*). We have also shown that, with synthetic modifications, amino sugars can even be compelled to bind the B-DNA major groove (*45−49*). Additionally, the ability of neomycin to assist oligodeoxynucleotide (ODN) delivery in cells (*50*) has led to the development of ODN−neomycin conjugates as sequence-specific nucleic acid binders (*51−53*). This establishes neomycin's versatility as a nucleic acid binder. We therefore explored if groove recognition of

*To whom correspondence should be addressed. E-mail: dparya@clemson.edu. Phone: 8646561106. Fax: 8646566617.
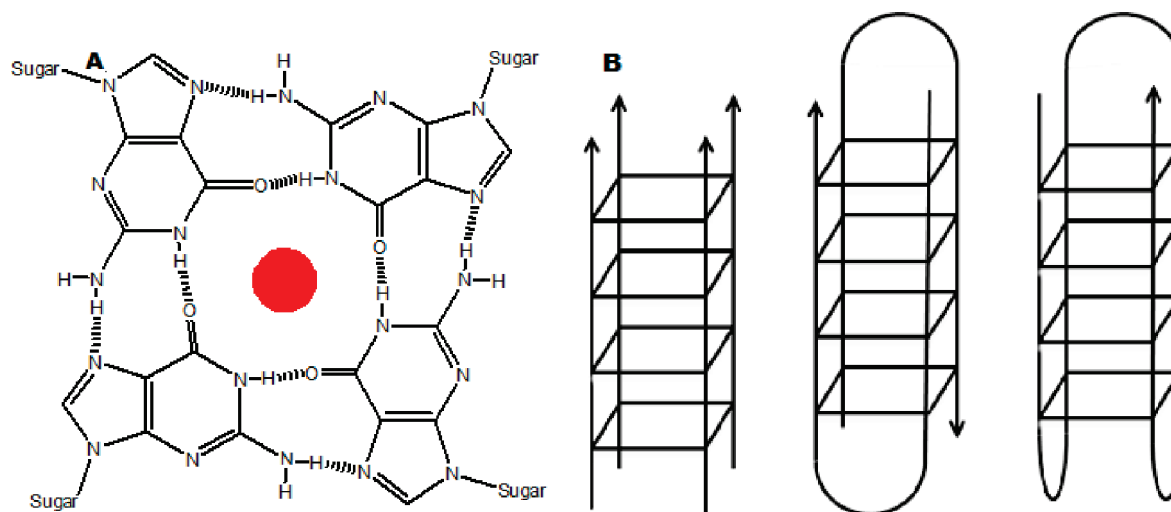
FIGURE 1: (A) Diagram of a G-tetrad showing the cyclic array of guanine bases connected by eight hydrogen bonds in Hoogsteen fashion. The cavity in the middle the tetrad is usually occupied by a monovalent or divalent cation represented by the ball in the figure. (B) Representative structures of two broad classes of quadruplexes based upon number of strands involved in their formation.
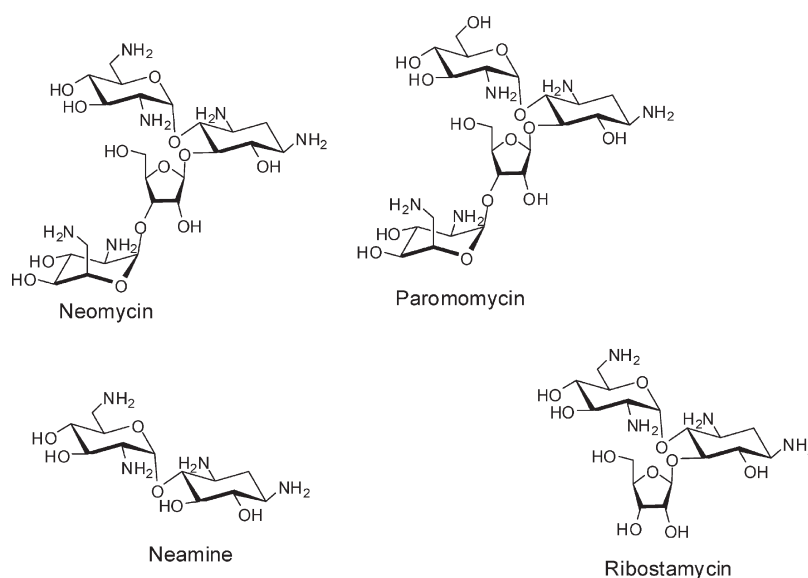

FIGURE 2: Structures of the ligands used in the study.

aminoglycosides could be extended to quadruplexes as different quadruplex grooves vary significantly in their width. The flexible nature of aminoglycosides makes them better candidates for groove recognition when compared to other DNA groove binders such as distamycin. Besides, quadruplex grooves vary greatly depending upon the structural forms (Figure 1B). For example, a tetramolecular parallel quadruplex has all identical, medium-sized grooves, while an antiparallel quadruplex can have grooves of all sizes (wide, medium, or narrow), all of which are considerably narrower than a B-DNA major groove. Neomycin in that context was of interest since it prefers to bind grooves that are narrower than B-form DNA major groove (A-form nucleic acid structures).

As a part of our exploration of groove recognition of nucleic acids, we report here that aside from its traditional targets like RNA, there is a considerable affinity of neomycin for G-quadruplex structures. Our studies showed a marked preference of aminoglycosides to the well-characterized *Oxytricha nova* (*O. nova*) telomeric sequence which is known to adopt an antiparallel quadruplex structure containing diagonal loop (*54*) which have been shown to play an important role in ligand

quadruplex interactions (*55, 56*). We have used ITC titration, CD titration, UV-melting, fluorescence titration, NMR, and computational methods to characterize the binding of neomycin and other aminoglycosides to *O. nova* telomeric quadruplex (Figure 2).

MATERIALS AND METHODS

Nucleic Acid Samples. All DNA oligonucleotides were purchased from IDT (Coraville, IA).

The concentrations of the DNA sample solutions were determined by measuring UV absorbance at 85 °C for the quadruplex-forming samples, while all other samples were measured at room temperature. Quadruplex structures were formed by heating the stock nucleotide solution in a buffer solution (either K^+ or Na^+) to 95 °C for 25 min and cooling back to room temperature.

The samples were then left to incubate at 4 °C for 2 days to 1 week. The oligomeric 12mer duplex (5′-dA$_{12}$-X-dT$_{12}$-3′) was synthesized on Expedite Nucleic Acid Synthesis System (8909) using standard phosphoramidite chemistry. Hexaethylene glycol was used as a spacer (denoted by -X- in the oligomeric DNA

sequence). The oligomers were purified on an anion-exchange HPLC column (Waters Gen-Pak FAX, 4.6 × 100 mm) with a Tris·HCl buffer system. Buffer A: 25 mM Tris·HCl, 1 mM EDTA, and 10% MeCN (v/v %). Buffer B: buffer A + 1 M NaCl. Conditions: 2−60% buffer B over buffer A during 0−16 min at a flow rate of 0.75 mL/min. All commercially obtained nucleic acids were used without further purification. The quadruplex formation was confirmed by CD spectroscopy and NMR.

Chemicals. Aminoglycosides used in the study were purchased from MP Biomedicals (Solon, OH). All chemicals were used without further purification.

Circular Dichroism Experiments. CD experiments were carried out at 20 °C using a Jasco J-810 spectropolarimeter with a thermoelectrically controlled cell holder. The CD spectra were recorded as an average of three scans. For CD titrations, a concentrated solution of the ligand was serially added to the nucleic acid sample and allowed to equilibrate for 5 min before a scan was taken. The resulting scan was plotted for CD signal changes with respect to wavelength. Data processing was done using Kaleidagraph 3.5 software.

Isothermal Titration Calorimetry (*ITC*) *Experiments*. ITC titrations were performed at 20.0 °C on a MicroCal VP-ITC (MicroCal, Inc., Northampton, MA). In most cases, small aliquots of ligand were injected (30 injections) from a rotating syringe with a stirring speed of 260 rpm into an isothermal sample chamber containing 1.42 mL of the quadruplex solution at 30 or 60 μM/strand. Each experiment was followed by a control experiment under the same conditions using buffer solution instead of the quadruplex. The buffer heats were then subtracted. The area under each heat burst curve was integrated, and the resulting data points were fitted using the Origin (version 5.0) software.

Fluorescent Intercalator Displacement (*FID*). Fluorescence experiments were performed on a Photon Technology International instrument (Lawrenceville, NJ) and on a TECAN Genois 96-well plate reader. All experiments were performed in a temperature range of 20−22 °C. The experiments were performed in a 3 mL quartz cell with 100 mM NaCl, 10 mM sodium cacodylate, and 0.5 mM EDTA buffer at pH 7.0 or with 200 μL total volume for 96-well plate experiments. The DNA solutions were prepared at 0.25 μM/quadruplex in 100 mM NaCl buffer and mixed with thiazole orange (TO) at 0.50 μM. The ligand was serially added to the DNA/TO solution and followed by a 4 min equilibration time before the fluorescence spectrum was recorded. The TO excitation was performed at 501 nm, and the emission was then recorded from 510 to 650 nm.

UV Spectroscopy. All UV spectra were obtained on a 12 cell holder Cary 1E UV−vis spectrophotometer equipped with temperature controller. Quartz cells with 1 cm path length were used for all the experiments. The quadruplex melting was monitored at 260, 235, and 295 nm wavelengths. The DNA samples were heated in the temperature range of 20.0−98.0 °C at the heating rate of 0.2 °C/min. The resulting temperature−absorbance profiles were plotted using Kaleidagraph 3.5 software. For T_m determination, first derivative analysis was used.

NMR Titrations. All NMR experiments were carried on a Bruker Avance (500 MHz) spectrophotometer equipped with z gradients and temperature control (Department of Chemistry, Clemson University NMR facility). The DNA concentration used in ^{1}H MNR titrations was 0.5 mM per strand. 2D NOESY experiments were carried out at a concentration of 2 mM per

strand and a final volume of 250 μL. All of the experiments were carried out in a Shimegi microvolume NMR tube matched with D$_2$O and collected at room temperature (∼295 K) or at 5 °C. All NMR samples contained 10 mM sodium phosphate, 0.5 mM EDTA, and 100 mM NaCl buffer at pH 7.0. Samples were prepared either as 90% H$_2$O + 10% D$_2$O or as 100% D$_2$O. For 1D water suppression, a pulse sequence with presaturation of HOD signal was used. For ^{1}H NMR experiments a total of 512 scans were collected. The data were visualized with Bruker X-Win Plot 3.5 software. For 2D NOESY experiments, a mixing time of 150, 200, and 250 ms was used; acquisition delay was 1.29 s. A total of 64 scans were collected. For NOESY experiments phase-sensitive water suppression was utilized as described by Sklenar (*57*). Data were subsequently 2D transformed and imported into SPARKY (*58*) for visualization and resonance assignment. DNA proton resonances were assigned based on NOE patterns and previously published chemical shifts (*59*, *60*).

Molecular Modeling. All dockings were performed as blind dockings (blind docking refers to the use of a grid box which is large enough to encompass any possible ligand−receptor complex) using Autodock Vina 1.0 (*61*). AutoDock Vina was chosen because of (a) its ability to take advantage of multiple core processors as well as its much more efficient search of the potential energy surface and (b) its high accuracy with ligands possessing more than 20 rotatable bonds when compared to Autodock 4.2.

Autodock Vina docking was performed using exhaustiveness value of 50. All other parameters were used as defaults. All rotatable bonds within the ligand were allowed to rotate freely, and the receptor was considered rigid. The Protein Data Bank file (PDB ID: 156D) (*62*) was used as the DNA quadruplex receptor for all dockings. All ligand structures were created using Discovery Studio Visualizer 2.5 and then brought to their energetically minimized structures by the Vega ZZ program (*63*) utilizing a conjugate gradient method with SP4 force field. Autodock Tools version 1.5.4 (*64*) was used to convert the ligand and receptor molecules to the proper file formats for AutoDock Vina docking. Validation that AutoDock Vina has the ability to identify the binding site and correctly score the receptor−ligand interactions was confirmed by its ability to accurately predict the differences among experimental binding constants for the series of aminoglycosides analyzed in this investigation. Further confidence is gained from AutoDock Vina's ability to produce dockings consistent with other available experimental data. Additionally, AutoDock Vina was used to confirm docking of neomycin to triplex DNA and successfully docked the ligand in the Watson−Hoogsteen groove as reported (*65*).

RESULTS AND DISCUSSION

Selection of Aminoglycosides as G-Quadruplex Binding Ligands. A recent study by Jarstfer and co-workers suggested aminoglycosides as a class of small molecules for telomerase inhibition (*66*). In addition to this, our initial findings suggested that aminoglycosides (neomycin specifically), apart from their preference for RNA targets, bind to DNA structures. Remarkable stabilization of triple helices of DNA, RNA, and hybrid structures prompted us to probe the common feature that makes neomycin bind such novel targets. Our studies suggested that aminoglycosides prefer to bind structures that adopt A-form (*44*) which are
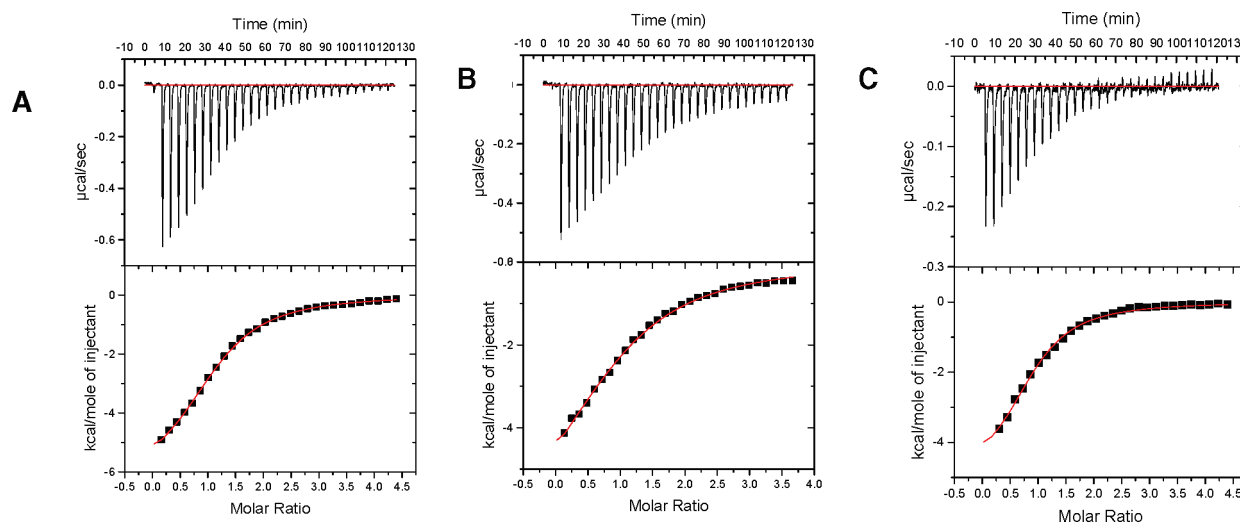
FIGURE 3: ITC profiles for the titration of *O. nova* quadruplex (GGGGTTTTGGGG)$_2$ with neomycin at 20 °C. (A) 10 mM sodium cacodylate, 0.5 mM EDTA, and 30 mM NaCl, pH 7.0. (B) 10 mM sodium cacodylate, 0.5 mM EDTA, and 100 mM NaCl, pH 7.0. (C) 10 mM sodium cacodylate, 0.5 mM EDTA, and 30 mM KCl, pH 7.0. The heat burst curves (top panels in the figures) are the result of 10 μL injections of a concentrated ligand solution into the DNA solution in buffer conditions as described earlier. The data points (lower panels of figure) reflect the corrected injection heats, which were obtained by subtracting the dilution heats obtained from separate control experiments in which ligand was titrated with buffer only. The red line represents the calculated fits of the data using one binding site model. The data fitting was carried out using Origin 5.0 software.

known for the narrowness of their major groove. Since G-quadruplex grooves can adopt varying sizes (narrow/medium/wide), which is dictated by the conformation of the base (*syn/anti*) participating in the G-tetrad formation, we have investigated if neomycin can possibly fit in the quadruplex grooves. Since neomycin lacks a group that can be detected by spectrophotometric techniques such as UV absorption or fluorescence, we have previously performed studies with ligands where a fluorescent probe (pyrene, acridine) conjugated to neomycin was used to find neomycin's preference for nucleic acid structures using competition dialysis experiments. The results indicated that, apart from its preference for binding to RNA, there is considerable binding of aminoglycoside to G-quadruplex structures as well, particularly antiparallel structure (*44*). We investigated the binding of neomycin to both parallel and antiparallel structure. Interesting binding properties were found with different types of antiparallel structures. Herein, we present a structurally well-characterized *O. nova* sequence, which is known to adopt an antiparallel structure (the findings of other sequences studied will be published elsewhere). The choice of this quadruplex was made since this quadruplex possesses three distinct types of grooves that quadruplex structures have been known to adopt.

ITC Titration of Neomycin into G-Quadruplex and Determination of Binding Parameters of Interaction. Isothermal calorimetry (ITC) has been one of the most sought after techniques for studying the interaction of biological molecules with ligands in recent years. This technique allows us to extract various thermodynamic parameters from a single experiment (*67−69*). We determined binding of *O. nova* (GGGGTTTTGGGG)$_2$ antiparallel quadruplex with two aminoglycosides, neomycin and paromomycin, using ITC. The affinities of the other aminoglycosides were too weak to obtain accurate thermodynamics using ITC. ITC titrations for this quadruplex with neomycin and paromomycin were carried out in sodium and potassium salt buffers. The binding constants (K_a) obtained from these titrations (Figures 3 and 4) are shown in Table 1 and the Supporting Information (S1). In the presence of both sodium and potassium salts, with increasing salt concentrations, a slight decrease in the

Table 1: Association Constants Obtained Using ITC Titration of *O. nova* Quadruplex (GGGGTTTTGGGG)$_2$ with Neomycin and Paromomycin under Different Salt Concentrations in Buffer 10 mM Sodium Cacodylate and 0.5 mM EDTA at pH 7.0 at 20 °C[a]

salt	ligand	salt conc (mM)	n (drug/tetraplex)	$K_a \times 10^5$ (M^{-1})
Na$^+$	neomycin	30	0.97 ± 0.08	3.79 ± 0.22
Na$^+$	neomycin	100	0.89 ± 0.01	1.03 ± 0.50
K$^+$	neomycin	30	1.34 ± 0.02	2.76 ± 0.21
K$^+$	neomycin	60	0.89 ± 0.02	1.42 ± 0.10
K$^+$	neomycin	90	0.77 ± 0.04	1.15 ± 0.08
K$^+$	paromomycin	60	1.34 ± 0.03	0.87 ± 0.04
K$^+$	paromomycin	90	1.07 ± 0.05	0.45 ± 0.01

[a]C values range from 1 to 11.3. c (Wiseman constant) = K_a[M]n, where K_a = association constant of the ligand, [M] = concentration of the macromolecule, and n = binding stoichiometry.

association constant was observed. In the presence of potassium ions, the association constant for the interaction decreased as the salt concentration increased from 30 to 90 mM. A similar effect in the association constant of neomycin to the quadruplex was observed in the presence of sodium ions as well. An almost 4-fold decrease occurred as the sodium salt concentration was varied from 30 to 100 mM. However, under similar salt conditions (30 mM), neomycin had a slightly higher affinity in the presence of sodium ions ($K_a = 3.79 \times 10^5$ M^{-1}), in comparison to potassium ions ($K_a = 2.76 \times 10^5$ M^{-1}).

In order to determine the number of ion pairs formed during the binding, a plot of log(K_a) versus log[K$^+$] was made (*70, 71*) (Figure 5). The slope from this log plot reveals the formation of one ion pair. This is in contrast to our findings for triple helical DNA (*72*) as well as previous work on binding of neomycin class antibiotics to the A-site rRNA construct where formation of three ion pairs was found (*73*). The formation of one ion pair thus suggests that binding occurs with less electrostatic interaction than what has been observed for the recognition of nucleic acid pockets in the aforementioned nucleic acids.
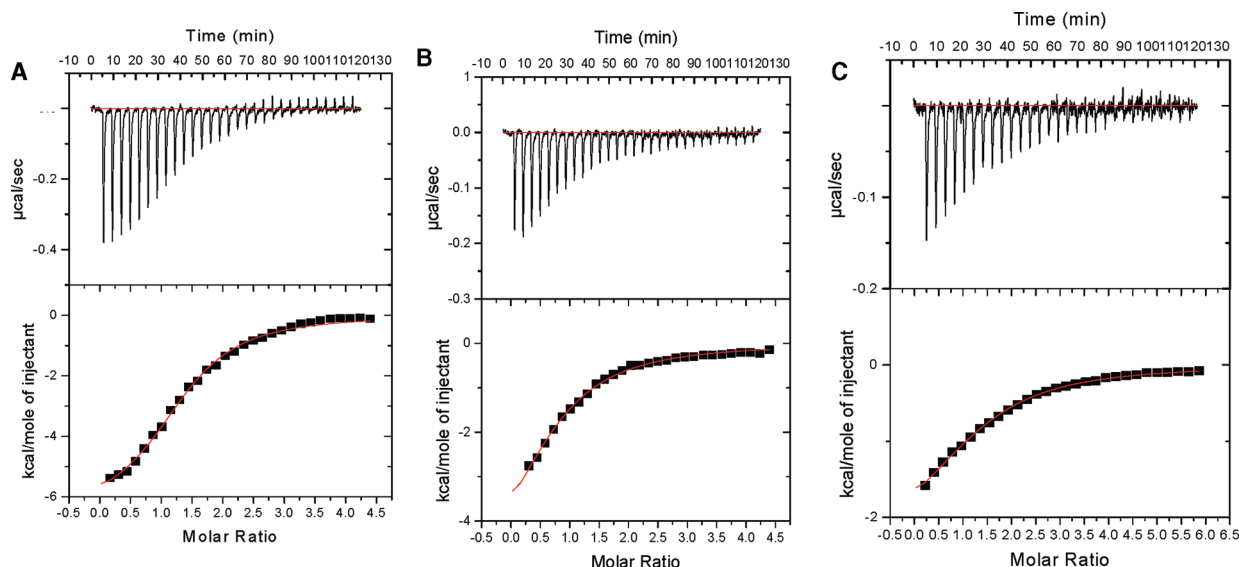
FIGURE 4: ITC profiles for the titration of *O. nova* quadruplex (GGGGTTTTGGGG)$_2$ with neomycin or paromomycin at 20 °C. (A) Neomycin in buffer 10 mM sodium cacodylate, 0.5 mM EDTA, and 60 mM KCl at pH 7.0. (B) Neomycin in buffer 10 mM sodium cacodylate, 0.5 mM EDTA, and 90 mM KCl at pH 7.0. (C) Paromomycin in buffer 10 mM sodium cacodylate, 0.5 mM EDTA, and 60 mM KCl at pH 7.0. The heat burst curves (top panel in the figures) are the result of 10 μL injections of a concentrated ligand solution into the DNA solution in buffer conditions as described earlier. The data points (lower panel in the figures) reflect the corrected injection heats, which were obtained by subtracting the dilution heats obtained from separate control experiments in which ligand was titrated with buffer only. The red line represents the calculated fits of the data using one binding site model. The data fitting was carried out using Origin 5.0 software.

The ITC titrations reveal close to a 1:1 binding stoichiometry (ligand to quadruplex) for both neomycin and paromomycin. This binding stoichiometry is of interest given that the quadruplex possesses three types of grooves. The solution structure of this quadruplex has revealed that two strands associate in an antiparallel fashion where thymine loops are diagonally connected (*54*). The bases around each tetrad are associated in a *syn-syn-anti-anti* fashion giving rise to a wide, two medium-sized, and a narrow groove (*60, 74*). We investigated the shape complementarity of neomycin and paromomycin to the different grooves of quadruplex. Previous studies have shown that neomycin does not stabilize B-DNA owing to wide B-DNA major groove (*45*); however, all four of the quadrupelx grooves are much shallower than a B-form DNA major groove. Additionally, and perhaps more importantly, there are two medium-sized grooves; a binding stoichiometry of two ligand molecules per quadruplex would be expected if binding were to occur to these grooves. Recognition of neomycin is thus likely in the narrow or wide groove present. The paromomycin binding also shows 1:1 binding stoichiometry which is suggestive of it binding to the same place as neomycin since the two aminoglycosides are structurally very similar, with neomycin possessing an extra amino group (Figure 2). A weaker binding of paromomycin is similar to observations previously reported, where neomycin shows a much higher increase in nucleic acid affinity than paromomycin (*30, 34*).

Fluorescent Intercalator Displacement Experiments. $^{G4}DC_{50}$ *values show neomycin is better than other aminoglycosides in G-quadruplex binding.* Fluorescent Intercalator displacement assay (FID) developed by Boger (*75, 76*) allows the study of nonfluorescent molecules binding to DNA. This assay has been extended to study the ligand binding to G-quadruplexes as well (*77, 78*).

We chose thiazole orange as our fluorescent probe. Thiazole orange is a more suitable probe than ethidium bromide, allowing determination of high-affinity sites, and thiazole orange shows little sequence-specificity (*75, 78*). Additionally, the fluorescence
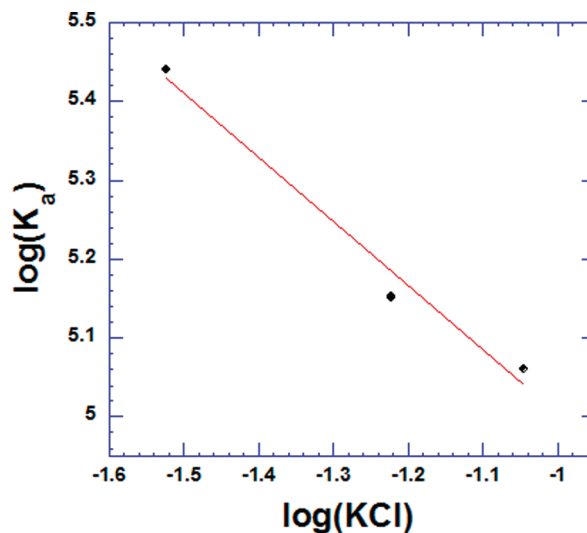

FIGURE 5: Salt dependence of the neomycin binding to *O. nova* quadruplex (GGGGTTTTGGGG)$_2$ in 10 mM sodium cacodylate and 0.5 mM EDTA at pH 7.0 (temperature 20 °C) at varying salt concentrations (30, 60, and 90 mM KCl, respectively). The experimental data were fit with linear regression, and the solid line reflects the resulting curve fit.

enhancement upon binding to DNA has been observed to be many fold higher for thiazole orange than ethidium bromide (*75*). Recently, the ability of a ligand binding to a G-quadruplex has been expressed in terms of $^{G4}DC_{50}$ values. These values are representative of ligand concentrations required to displace 50% of the probe bound to the G-quadruplex target in the displacement assays. To ascertain the ratio of fluorescent probe bound to DNA, we carried direct fluorescence titrations where thiazole orange was titrated with concentrated quadruplex DNA solution. The titration revealed that thiazole orange binds to DNA in 2:1 stoichiometric ratio (Figure 6A,B). A DNA solution containing 2 equiv of thiazole orange was first titrated with the appropriate ligand solution
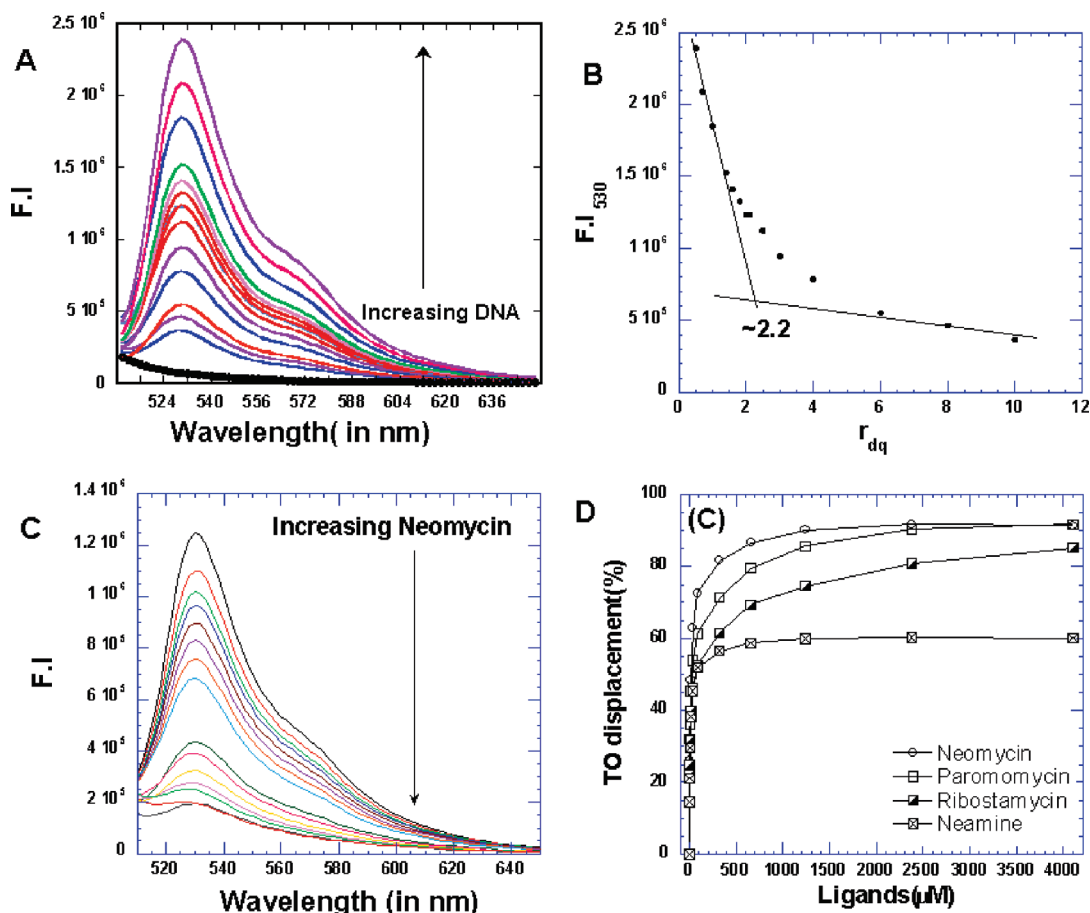
FIGURE 6: (A) Fluorescence titration of thizaole orange with quadruplex DNA (GGGGTTTTGGGG)$_2$. The thiazole orange solution was titrated with the concentrated DNA solution. (B) The binding stoichiometry plot of thizaole orange with quadruplex DNA. r$_{dq}$ refers to the ratio of ligand to quadruplex. (C) A representative FID displacement titration showing the displacement of fluorescent probe with the addition of concentrated aminoglycoside (neomycin) from the bound quadruplex DNA. (D) The graph showing the displacement of thiazole orange from quadruplex DNA using different aminoglycosides. All experiments were performed in buffer 10 mM sodium cacodylate, 0.5 mM EDTA, and 100 mM NaCl at pH 7.0 (T = 20 °C).

displacing the bound thiaozle orange. As increasing amounts of ligand were added, the fluorescence intensity continued to decrease, suggesting displacement of bound thiazole orange (Figure 6C). To see if the fluorescence quenching was, indeed, an outcome of aminoglycoside binding, control experiments were run. Titration of thiazole orange with neomycin did not cause any significant drop in the fluorescence intensity. In addition to this, a polyamine, spermine, was titrated to displace bound thiazole orange (Figure S2; see Supporting Information). Even after addition of large amounts of polyamine, extremely poor thiazole orange displacement resulted. These findings indicate that fluorescence quenching of the probe, thiazole orange, is not the outcome of nonspecific interactions. Among the aminoglycosides studied, neomycin clearly showed the least amount of ligand required to displace 50% of fluorescent probe. The order of quadruplex preference for four aminoglycosides studied was found to be neomycin > paromomycin > ribostamycin > neamine (Table 2, Figure 6D) (please see Supporting Information). The DC$_{50}$ value obtained for this experiment showed clear preference of neomycin for quadruplex (at least 4-fold higher) than its affinity to duplex DNA. The other aminoglycosides showed even higher DC$_{50}$ values for duplexes. For quadruplex, the neomycin DC$_{50}$ (16.6 μM) is almost 2-fold lower than paromomycin (29.1 μM) and approximately 4.5-fold lower than ribostamycin DC$_{50}$ (68 μM). A much larger difference is seen with aminoglycoside binding to the DNA triplex, with neomycin preference DC$_{50}$ (13 μM) almost 15-fold less than paromomycin

Table 2: DC$_{50}$ Values Obtained from Studies on Duplex and Quadruplex DNAs

aminoglycoside	(GGGGTTTTGGGG)$_2$ DC$_{50}$ (μM)	5′A$_{12}$-X-T$_{12}$-3′ DC$_{50}$ (μM)
neomycin	16.6 ± 2.0	68.2 ± 4.0
paromomycin	29.1 ± 5.0	328.1 ± 64.2
ribostamycin	68.1 ± 16.0	1037.9 ± 193.0
neamine	79.0 ± 24.0	520.7 ± 244.4

DC$_{50}$ (157 μM), and about 35-fold lower than ribostamycin DC$_{50}$ = (459 μM) as observed for the 5′-dA$_{12}$-X-dT$_{12}$-X-dT$_{12}$-3′ triplex (*72*). While the relative affinities of the drugs to the same target can be compared using this method, one should be cautious in comparing drug binding to different targets, as slight differences in affinities of thiazole orange to duplex DNA, triplex DNA, and quadruplex DNA can complicate the analysis. A closer look at the relative affinities of aminoglycosides reveals the same general trend where neomycin was found to have least DC$_{50}$ value. The findings presented here correlate very well with the ability of these ligands for telomerase inhibition where neomycin was identified as best of all aminoglycosides studied (*66*).The results presented in Table2 show an increasing DC$_{50}$ value with decreasing charge on the aminoglycoside, suggesting that the charge present on them plays a role in their affinity to the quadruplex. However, association constants obtained in increasing salt concentrations displayed little
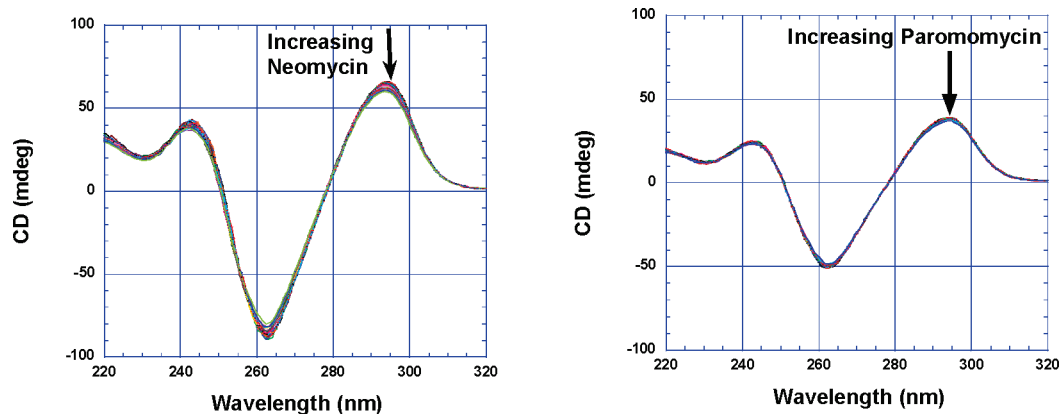
FIGURE 7: CD titration of (GGGGTTTTGGGG) $_2$ quadruplex with neomycin (left) and paromomycin (right) in buffer 10 mM sodium cacodylate and 100 mM NaCl at pH 7.0. Small aliquots of ligand were serially added to the DNA solution at 20 °C. The DNA concentration used in neomycin titration was 15 μM/str. The DNA concentration used in paromomycin titration was 10 μM/str. During the titration, the DNA solution was stirred with the added ligand for 5 min followed by another 5 min of equilibration time. The CD signal represents an average of three scans.

variations in the binding affinity of neomycin. Given that salt dependence studies indicate less charge interactions (formation of three ion pairs for triplex DNA while one ion pair formation for quadruplex DNA) than triplex DNA, shape complementarity seems more likely for quadruplex groove in comparison to triplex DNA or A-site RNA. This is in contrast to the triplex groove recognition by aminoglycosides where both charge/potential complementarity play a significant role in binding.

The difference between neomycin and paromomycin is one positive charge, and the binding studies indicate that this positive charge (amine) leads to a 2-fold increase in neomycin binding to the quadruplex and a 15-fold increase in neomycin binding to the triplex. Additionally, as seen with the salt dependence studies, very little dependence on salt is seen with aminoglycoside binding to quadruplex (one ion pair) as opposed to three ion pairs seen with neomycin bound to a DNA triplex. One can infer that shape complementarity (as opposed to potential complementarity) plays a larger role in aminoglycoside-based recognition of the quadruplex grooves, when compared to their binding to the DNA triplex grooves.

CD Spectroscopy. We carried out complete CD titrations to find out ligand-induced changes in the CD signal to observe any conformation change accompanying the ligand binding. The CD titration of the *O. nova* quadruplex, (GGGGTTTTGGGG)$_2$, was carried in the presence of aminoglycosides (Figure 7). The maxima of the CD signals in all experiments carried out were observed at ~295 nm while the minimum is at ~260 nm. This is consistent with the antiparallel structure of the G-quadruplex (*79*). However, binding of neomycin induces minimal CD changes (Figure 7 (left)) in the DNA absorption region even after addition of large amounts of ligand (more than 3 equiv). A similar CD pattern was also observed for paromomycin (Figure 7 (right)). These CD results suggest that interaction of these ligands does not perturb the quadruplex structure.

UV Thermal Denaturation Studies. UV thermal melting experiments were carried out to find any ligand-induced thermal stabilization. The *O. nova* quadruplex melted at 55.7 °C in cacodylate buffer containing 100 mM sodium salt. Quadruplex was thermally denatured with aminoglycosides. At 1:1 ligand to quadruplex ratio, the thermal denaturation profiles showed ~1−2 °C stabilization in the presence of neomycin (Figures 8 and S3; see Supporting Information). Similar affinities with DNA triplex lead to > 10 °C changes in triplex denaturation tempera-
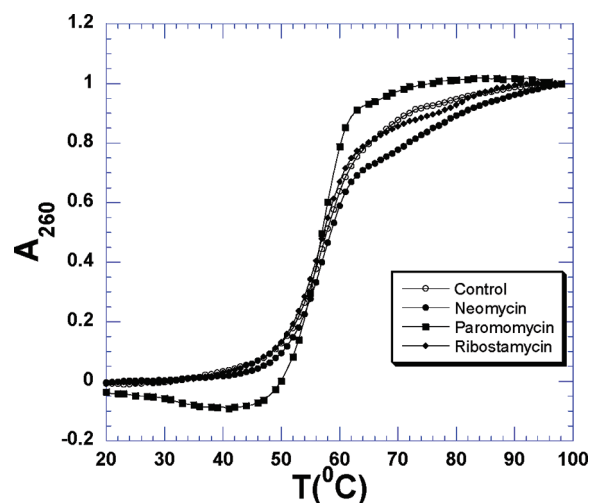

FIGURE 8: UV melting profiles of *O. nova* quadruplex (GGGGTTT-TGGGG)$_2$ in the presence of various ligands. The oligonucleotides concentration was 10 μM/str while the ligand concentrations were 1:1 quadruplex:ligand ratio in buffer 10 mM sodium cacodylate, 0.5 mM EDTA, and 100 mM NaCl at pH 7.0. The nucleic acid samples were heated at the rate of 0.2 deg/min. The melting temperatures were determined by the first derivative analysis.

tures. We probed these, somewhat, surprising thermal melting profiles by studying the binding of neomycin at increased temperatures using ITC. In potassium buffer, a general decreasing trend in the association constant was observed as temperature was raised. Almost 4-fold decrease in the association constant was determined as the temperature of the study was increased from 20 to 40 °C (Figure S4 and Table S1; see Supporting Information). In the sodium buffer, when we carried the ITC experiment at 40 °C, weak and broad heat burst curves were obtained. The resulting enthalpy profile could not be fitted. Because of these limitations, the association constant close to melting temperatures could not be determined. The ITC titrations at different temperatures in potassium buffer suggest a weakened binding at temperatures close to the melting point of the DNA. Additionally, we also probed the thermal melting profile of neomycin binding to quadruplex by van't Hoff's method using procedures described by Mergny (*80, 81*) and Chaires (*73*). The thermodynamic data were obtained at 1:1 quadruplex to ligand ratio. The neomycin binding was found to be enthalpically favored (as compared to DNA melting alone) by
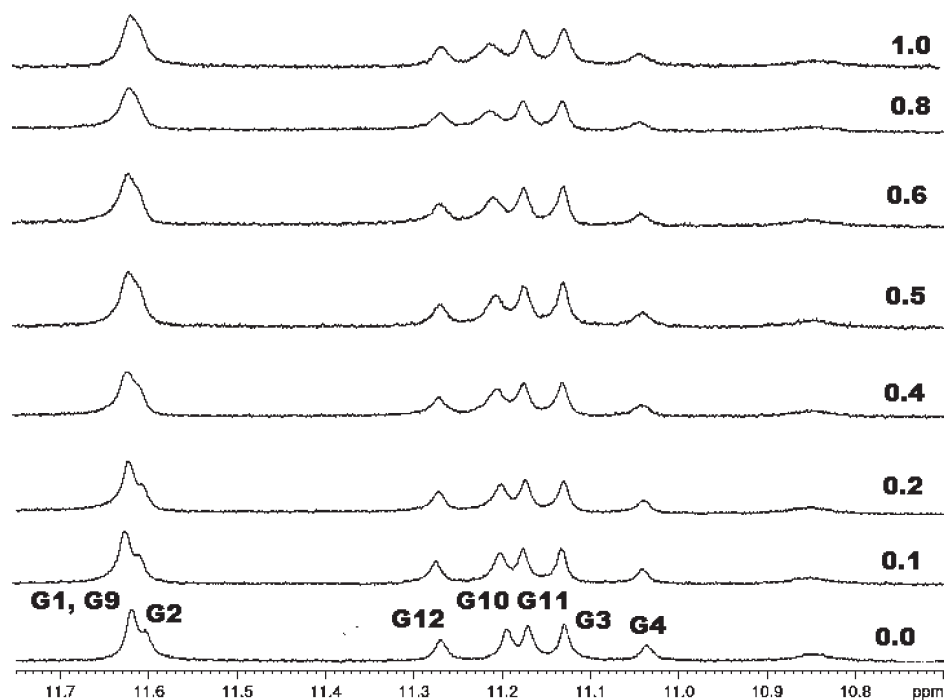
FIGURE 9: ¹H NMR titration of *O. nova* quadruplex DNA with paromomycin. Increasing amounts of the ligand were serially added to the DNA solution as indicated on each scan. The DNA solution was prepared in 10 mM sodium phosphate, 0.5 mM EDTA, and 100 mM NaCl at pH 7.0. The titration was carried out at room temperature (22 °C).

Table 3: Thermodynamic Parameters of Melting of (GGGGTTTTGGGG)₂ Quadruplex in Buffer 10 mM Sodium Cacodylate, 0.5 mM EDTA, and 100 mM NaCl at pH 7.0[a]

ligand	ΔH (kcal/mol)	ΔS (cal/mol)	ΔG (kcal/mol) at 55 °C
none	−133.36	−380.55	−8.49
neomycin (1:1)	−134.20	−382.7	−8.62

[a][DNA] = 5 μM/strand. Please see Supporting Information for additional details for calculation of thermodynamic parameters.

−0.84 kcal·mol⁻¹ (Table 3), whereas the Gibbs free energy for the quadruplex dissociation was favored by −0.13 kcal·mol⁻¹ at 55 °C. This small favorable dissociation of the quadruplex again shows that binding of neomycin is weak/negligible at temperatures close to the melting temperatures of the quadruplex.

Another interesting aspect of neomycin binding to the quadruplex is the sharpness of the melting profile as compared to the melting of DNA alone (consistent with multiple trials). A sharper transition is indicative of a strongly temperature dependent affinity constant (*80*) which is concurrent with our findings from ITC measurements.

NMR Studies with Paromomycin and Neomycin. The solution structure of the *O. nova* is well established having been solved in both sodium and potassium salt solutions. Both the sodium and potassium forms of the structure have the same overall fold with slight local variations in the T4 loop (*59, 60*). To investigate the binding of neomycin and paromomycin to quadruplex DNA, the DNA sample was prepared in similar conditions as employed in other biophysical experiments. The chemical shifts for the imino, amino, and aromatic protons were assigned using procedures described by Feigon and co-workers (*54, 59, 60*). The ¹H NMR titration was initially carried out with increasing amounts of neomycin. However, even at low ligand concentration (0.5 mol equiv of ligand to DNA) considerable precipitation was seen. We, therefore, carried out ¹H NMR titration with

structurally similar ligand paromomycin. ITC experiments with paromomycin indicated a slightly lower binding to our DNA target yet demonstrated the same stoichiometry as neomycin. Given its nearly identical structure (the difference being an amino group) as neomycin, we hypothesized a similar mode of binding as what would be expected with neomycin. No precipitation was seen with paromomycin titration into the DNA up to 1.0 mol equiv of the ligand. The addition of the paromomycin to the DNA caused both shifts in individual resonance positions as well as broadening of the chemical shifts in both imino and aromatic regions of protons. Figure 9 shows the representative titration of paromomycin into DNA.

Several proton resonances demonstrated shifts in both imino and aromatic regions of proton spectra as shown in Figure 9. The chemical shift positions of both imino and aromatic protons of G2 showed the greatest change (Figure 10). The other major shifts were observed for G3, G4, and G10. The G10 imino protons were broadened as well. Interestingly, thymine bases that make the loop in this DNA structure showed little effect on them upon paromomycin titration. Titrations with neomycin also showed similar shifts until precipitation was seen (Figure S5; see Supporting Information). However, broadening of the imino resonances was more prominent in comparison to paromomycin. To further characterize the mode of binding of paromomycin to DNA, 2D NOESY experiments will be performed, and such a structural elucidation of ligand−quadruplex complex is now underway. While a comprehensive analysis is needed to completely characterize the structure of the complex, these initial results clearly demonstrate the binding of paromomycin to DNA in a single stable conformation.

Looking at the groove structures of the four grooves of the quadruplex, the wide groove is composed of bases (G1-G4)-(G4-G1) while the two medium grooves are composed of bases (G1-G4)-(G9-G12) (G4-G1)-(G12-G9) and the minor groove involves (G9-G12)-(G12-G9) bases. Most of the changes in the chemical
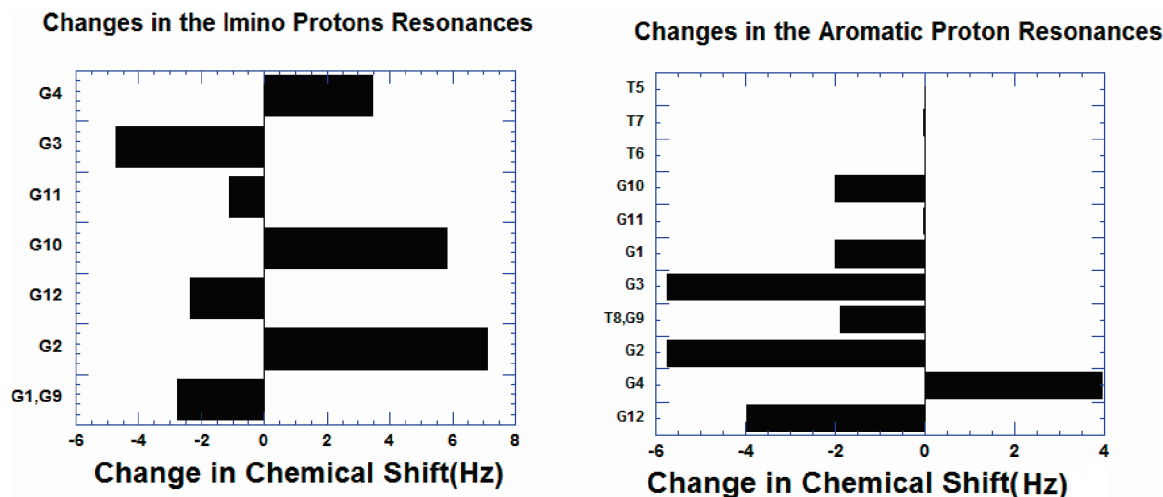
Changes in the Imino Protons Resonances

Changes in the Aromatic Proton Resonances

FIGURE 10: Changes in the proton resonances at 1:1 DNA:ligand ratio of ^{1}H NMR titration of *O. nova* with paromomycin. The changes observed in the imino proton resonances are shown on the left, and changes in the aromatic proton resonances are presented on the right.

Table 4: Binding Energies Obtained from Docking of Neomycin and Paromomycin in the Different Grooves of the Quadruplex DNA Studied

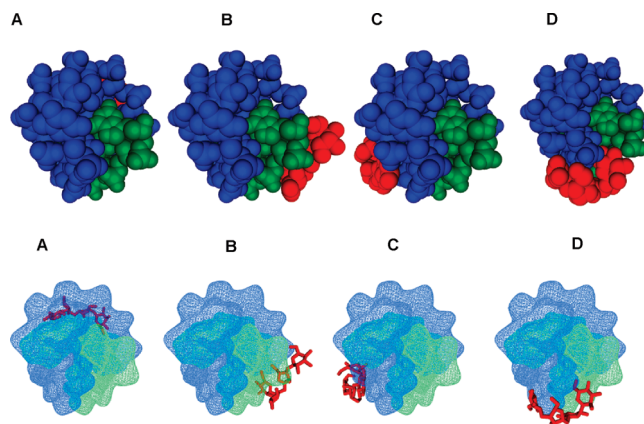| aminoglycoside	groove	E_{dock} (kcal·mol^{-1})
neomycin	narrow	−4.0
neomycin	medium (1)	−5.4
neomycin	medium (2)	−5.4
neomycin	wide	−7.2
paromomycin	wide	−7.0

FIGURE 11: Computer-generated models showing two different views of neomycin (red) bound to four different grooves of the *O. nova*: (A) neomycin docked in the wide groove; (B) neomycin docked in the narrow groove; (C, D) neomycin docked in the two medium grooves.

shifts of imino and aromatic protons are centered on G1-G4 bases which comprise the wide groove of the quadruplex, suggesting that the drug binding significantly perturbs the wide groove of the quadruplex, as opposed to the other grooves.

Docking Studies. There has been an increasing interest in using docking methods which allow rapid selection of promising candidates from drug libraries (*29, 82*). AutoDock, initially designed to study protein interactions, has been used to study small molecule−nucleic acid interactions revealing accurate reproducibility of crystal structures for both groove binders and intercalators bound to nucleic acids (*83*). Few laboratories have also benefited from the use of AutoDock for probing small molecule interactions with the G-quadruplex (*29, 84, 85*). We have performed docking studies using recently introduced AutoDock Vina. According to the molecular modeling performed in this study, neomycin shows marked preference for the wide groove of the *O. nova* quadruplex as compared to the two medium-sized grooves and the narrow groove (Table 4, Figure 11).

When bound to the quadruplex, neomycin can adopt four different conformations that are identical in energy due to the symmetry of the quadruplex's widest groove. These conformations all share the following characteristics (*1*). All rings are essentially parallel to the groove floor except for ring I (*2*). In each conformation there exists either one close electrostatic interaction (<3.5 Å), consistent with the experimentally determined salt dependence studies (formation of one ion pair), or two more distant contacts (<4.5 Å) (*3*). Each low-energy conformation resides in the wide groove (*4*). Every conformation has approximately the same energy (−7.2 kcal·mol^{-1}) according to the AutoDock Vina scoring function.

The poses for neomycin have been divided into four archetypes (Figure 12). Within these archetypes there is a great deal of

flexibility favoring increased electrostatics, van der Waals, or hydrogen-bonding interactions.

We also carried out similar docking studies with paromomycin (Figure 13). As expected, due to the structural similarity (Figure 2) between paromomycin and neomycin, the observed low-energy binding pocket is also the wide groove of the quadruplex. In comparison to neomycin binding to the quadruplex, it is energetically disfavored by 0.2 kcal·mol^{-1} (Table 4), corroborating the findings from our calorimetric studies. The absence of one amine group, as compared to neomycin, leads to two low-energy confirmations possible for paromomycin, as opposed to four in the case of neomycin.

Neomycin's unfavorable interaction in the narrow groove of the quadruplex likely stems from the extreme narrowness of the groove (end to end distance <4.5 Å). Few reports of quadruplex groove binding ligands have been reported (*29*). It has been suggested that the quadruplex groove recognition is expected to give a higher degree of selectivity over the other DNA structures, yet few groove binders have been identified (*29*). Polyamides such as distamycin have been shown to bind as two sets of stacked dimers in two of the four identical grooves of (TGGGGT)$_4$ parallel quadruplex (*27*) with much lower affinities than the
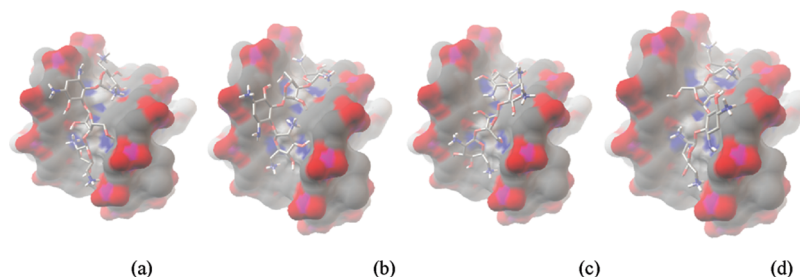
FIGURE 12: Computer-generated model showing the four docked poses of neomycin to quadruplex where (a)−(d) represent the four poses of equal energy available to neomycin. Binding affinity is −7.2 kcal·mol^{-1}.
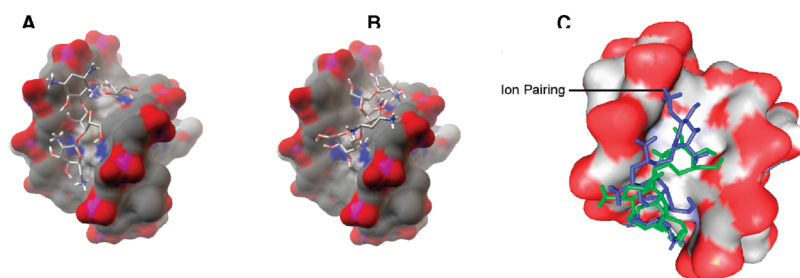

FIGURE 13: Computer-generated models showing paromomycin bound to quadruplex. (A) and (B) demonstrate the two poses available to paromomycin in the wide groove. Binding affinity is −7.0 kcal·mol^{-1}. (C) A computer-generated model showing neomycin (blue) and paromomycin (green) viewed together in the wide groove. Ion pairing interaction of neomycin to phosphate backbone is shown by the solid black line.

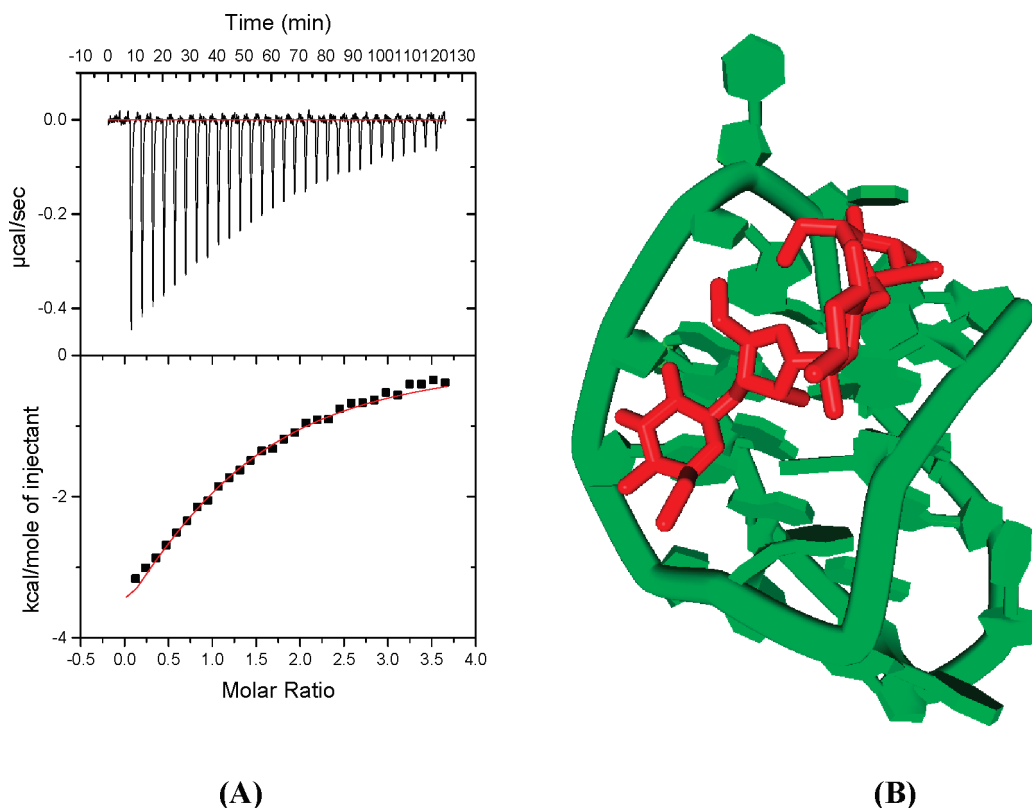**(A)**   **(B)**

FIGURE 14: (A) ITC titration of neomycin into human telomeric quadruplex DNA in buffer 100 mM NaCl, 0.5 mM EDTA, and 10 mM sodium cacodylate at pH 7.0 (T = 20 °C). (B) Computer model of neomycin binding in the wide groove of 22mer DNA sequence d-(5′-AGGGTTAGGG-TTAGGGTTAGGG-3′) mimicking the human telomeric end. The DNA is shown in green, and neomycin is shown in red.

duplex. Aminoglycoside-based shape complementarity to the quadruplex large groove opens up new avenues for selective groove recognition of the quadruplexes.

We also carried out docking studies of neomycin binding another antiparallel quadruplex formed by the DNA sequence (AGGGTTAGGGTTAGGGTTAGGG) mimicking the human telomeric end. This quadruplex, like the (GGGGTTTTGGGG)$_2$ quadruplex, also has four grooves (narrow, medium, and wide) as revealed by its solution NMR structure (*86*). ITC experiments with this DNA quadruplex with neomycin revealed a 1:1 binding stoichiometry which is the same as observed with the *O. nova* quadruplex (Figure 14A, Supporting Information Table S2).
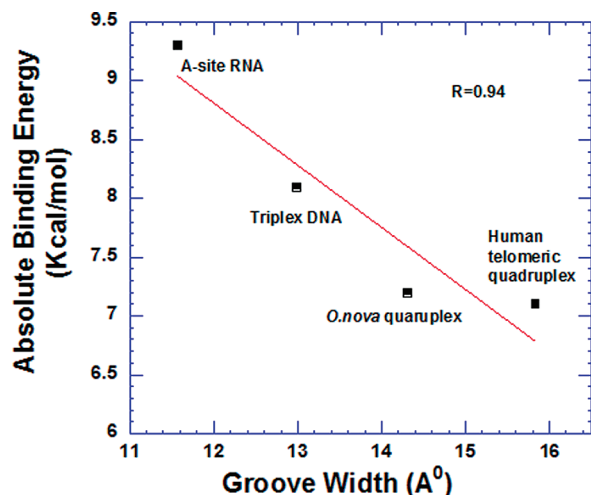
FIGURE 15: A graph showing the AutoDock Vina derived binding affinity of neomycin to different nucleic acids with respect to the widths of their binding sites. (Please see Supporting Information for PDB ID of nucleic acids used in the study and Table S3.)

The docking studies showed that similar to *O. nova* the most favorable binding pose had neomycin in the middle of the wide groove (Figure 14B). However, the affinity of neomycin to this quadruplex is lower than neomycin's affinity to the *O. nova* quadruplex (please see Supporting Information).

This result also suggests that binding of neomycin is probable in the wide groove quadruplex DNA−DNA structures (as opposed to medium/narrow grooves). To compare the dependence of ligand binding to nucleic acid groove widths, AutoDock analysis of groove binding of neomycin to different nucleic acids was also performed. The results from this analysis are presented in Figure 15.

A linear correlation between groove width and neomycin binding was seen. There is a decrease in binding affinity with increasing groove width indicating that neomycin binding to different DNA structures is clearly groove width dependent. As grooves get wider (from A-site RNA to triplex DNA to quadruplex DNA), decrease in the shape complementarity of ligand−nucleic acid leads to a decrease in affinity.

CONCLUSION

The recent advances in the G-quadruplex recognition by small molecules have prompted us to explore the groove binding nature of aminoglycosides. From our studies, the following conclusions can be drawn:

(1) Neomycin binds *O. nova* quadruplex in 1:1 binding stoichiometry. The direct ITC titration of the *O. nova* quadruplex DNA revealed that neomycin binds with association constants $K_a \sim 10^5$ M^{-1} in the presence of both sodium and potassium ions. The ligand favors the *O. nova* quadruplex over the 22mer human telomeric quadruplex.

(2) The salt dependence studies in the presence of both sodium and potassium ions showed the same trend of a slight decrease in the association constants with an increase in the salt concentrations. This indicates that the binding interaction of neomycin to the quadruplex is moderately driven by electrostatic interactions. The binding stoichiometry of 1:1 is indicative of a single unique site for neomycin complexation.

(3) FID assays were conducted with the *O. nova* quadruplex. The binding of fluorescent probe indicated a 2:1 ratio of ligand to quadruplex binding. The $^{G4}DC_{50}$ values obtained from FID

titrations show that neomycin is best in displacing the fluorescent probe bound to quadruplex. The other aminoglycosides were much worse in displacing the fluorescent probe bound to these quadruplexes. Neomycin binds approximately 5-fold better than ribostamycin.

(4) The binding mode of neomycin does not perturb the structure of the quadruplex. The CD experiments showed that binding of either neomycin or any other aminoglycoside brings negligible change in the CD signal.

(5) The binding of ligands is accompanied by small thermal stabilization under the buffer conditions used. UV melting studies show that complexation of any of the ligands studied results in small increase in the melting temperature of the quadruplex DNA due to decreased binding at temperatures near the melting point of the DNA.

(6) ^1H NMR titration of the quadruplex DNA with paromomycin suggests ligand binding in the wide groove.

(7) A molecular model generated using AutoDock Vina corroborates the experimental results, suggesting that neomycin binds to the wide quadruplex groove with one amino group forming an ion pair with quadruplex phosphate negative charge.

Recognition of quadruplex nucleic acids has mostly been achieved using planar aromatic ligands through stacking interactions. This has been an outcome of lack of structures that could bind in the quadruplex grooves. With the availability of groove binding aminosugars, quadruplex groove recognition can now be utilized and coupled with ligands that are known to bind through stacking interactions. We have successfully demonstrated that such coupling of two moieties leads to increased binding than individual units for triplex, duplex, and hybrid nucleic acid structures (*36, 40, 44*). It is probable that such high-affinity ligands for specific binding to quadruplexes can be generated by combining two ligands that have their own distinct binding sites. Such efforts are currently underway in our laboratories and will be reported in the near future.

SUPPORTING INFORMATION AVAILABLE

ITC titration data, UV thermal denaturation profiles, and NMR spectra of neomycin titration with the quadruplex. This material is available free of charge via the Internet at http://pubs.acs.org.

REFERENCES

1. Mergny, J. L., and Helene, C. (1998) G-Quadruplex DNA: A Target for Drug Design. *Nat. Med. (N. Y., NY, U. S.) 4*, 1366–1367.
2. Neidle, S., and Read, M. A. (2000) G-Quadruplexes as Therapeutic Targets. *Biopolymers 56*, 195–208.
3. Perry, P. J., and Jenkins, T. C. (2001) DNA Tetraplex-Binding Drugs Structure-Selective Targeting is Critical for Antitumour Telomerase Inhibition. *Mini Rev. Med. Chem. 1*, 31.
4. Riou, J. F., Gomez, D., Morjani, H., and Trentesaux, C. (2006) in *Quadruplex Ligand Recognition: Biological Aspects* (Neidle, S., and Balasubramanian, S., Eds.) pp 154−179, The Royal Society of Chemistry, Cambridge, UK.
5. Oganesian, L., and Bryan, T. M. (2007) Physiological Relevance of Telomeric G-Quadruplex Formation: A Potential Drug Target. *BioEssays 29*, 155–165.

6. Camarena, F. S., Serral, G. C., and Santalo, F. S. (2007) Telomerase and Telomere Dynamics in Ageing and Cancer: Current Status and Future Directions. *Clin. Transl. Oncol. 9*, 145–154.

7. Helder, M. N., Wisman, G. B. A., and Van der, Z. (2002) Telomerase and Telomeres: From Basic Biology to Cancer Treatment. *Cancer Invest. 20*, 82–101.

8. Kelland, L. R. (2001) Telomerase: Biology and Phase I Trials. *Lancet Oncol. 2*, 95–102.

9. Kelland, L. (2007) Targeting the Limitless Replicative Potential of Cancer: The Telomerase/Telomere Pathway. *Clin. Cancer Res. 13*, 4960–4963.

10. Autexier, C., and Lue, N. F. (2006) The Structure and Function of Telomerase Reverse Transcriptase. *Annu. Rev. Biochem. 75*, 493–517.

11. Monchaud, D., and Teulade-Fichou, M. P. (2008) A Hitchhiker's Guide to G-Quadruplex Ligands. *Org. Biomol. Chem. 6*, 627–636.

12. Burge, S., Parkinson, G. N., Hazel, P., Todd, A. K., and Neidle, S. (2006) Quadruplex DNA: Sequence, Topology and Structure. *Nucleic Acids Res. 34*, 5402–5415.

13. Parkinson, G. N. (2006) Fundamentals of Quadruplex Structures, in *Quadruplex Nucleic Acids* (Neidle, S., and Balasubramanian, S., Eds.) pp 1−30, Royal Society of Chemistry, Cambridge, U.K.

14. Hud, N. V., and Plavec, J. (2006) The Role of Cations in Determining Quadruplex Structure and Stability, in *Quadruplex Nucleic Acids* (Neidle, S., and Balasubramanian, S., Eds.) pp 100−130, The Royal Society of Chemistry, Cambridge, UK.

15. Sun, D., Thompson, B., Cathers, B. E., Salazar, M., Kerwin, S. M., Trent, J. O., Jenkins, T. C., Neidle, S., and Hurley, L. H. (1997) Inhibition of Human Telomerase by a G-Quadruplex-Interactive Compound. *J. Med. Chem. 40*, 2113–2116.

16. Ping Wang, L. R., He, Hanping, Liang, Feng, Zhou, Xiang, and Tan, Zheng (2006) A Phenol Quaternary Ammonium Porphyrin as a Potent Telomerase Inhibitor by Selective Interaction with Quadruplex DNA. *ChemBioChem 7*, 1155–1159.

17. Seenisamy, J., Bashyam, S., Gokhale, V., Vankayalapati, H., Sun, D., Siddiqui-Jain, A., Streiner, N., Shin-ya, K., White, E., Wilson, W. D., and Hurley, L. H. (2005) Design and Synthesis of an Expanded Porphyrin that has Selectivity for the c-MYC G-Quadruplex Structure. *J. Am. Chem. Soc. 127*, 2944–2959.

18. Wei, C., Jia, G., Yuan, J., Feng, Z., and Li, C. (2006) A Spectroscopic Study on the Interactions of Porphyrin with G-Quadruplex DNAs. *Biochemistry* (*New York*) *45*, 6681–6691.

19. Hounsou, C., Guittat, L., Monchaud, D., Jourdan, M., Saettel, N., Mergny, J. L., and Teulade-Fichou, M. P. (2007) G-Quadruplex Recognition by Quinacridines: A SAR, NMR, and Biological Study. *ChemMedChem 2*, 655–666.

20. Zagotto, G., Sissi, C., Moro, S., Ben, D. D., Parkinson, G. N., Fox, K. R., Neidle, S., and Palumbo, M. (2008) Amide Bond Direction Modulates G-Quadruplex Recognition and Telomerase Inhibition by 2,6 and 2,7 Bis-Substituted Anthracenedione Derivatives. *Bioorg. Med. Chem. 16*, 354–361.

21. Waller, Z. A. E., Shirude, P. S., Rodriguez, R., and Balasubramanian, S. (2008) Triarylpyridines: A Versatile Small Molecule Scaffold for G-Quadruplex Recognition. *Chem. Commun.* (*Cambridge, U.K.*)*, 1467–1469.

22. Jantos, K., Rodriguez, R., Ladame, S., Shirude, P. S., and Balasubramanian, S. (2006) Oxazole-Based Peptide Macrocycles: A New Class of G-Quadruplex Binding Ligands. *J. Am. Chem. Soc. 128*, 13662–13663.

23. Fu, B., Huang, J., Ren, L., Weng, X., Zhou, Y., Du, Y., Wu, X., Zhou, X., and Yang, G. (2007) Cationic Corrole Derivatives: A New Family of G-Quadruplex Inducing and Stabilizing Ligands. *Chem. Commun.*, 3264–3266.

24. Brassart, B., Gomez, D., Cian, A. D., Paterski, R., Montagnac, A., Qui, K. H., Temime-Smaali, N., Trentesaux, C., Mergny, J. L., Gueritte, F., and Riou, J. F. (2007) A New Steroid Derivative Stabilizes G-Quadruplexes and Induces Telomere Uncapping in Human Tumor Cells. *Mol. Pharmacol. 72*, 631–640.

25. Franceschin, M., Rossetti, L., D'Ambrosio, A., Schirripa, S., Bianco, A., Ortaggi, G., Savino, M., Schultes, C., and Neidle, S. (2006) Natural and Synthetic G-Quadruplex Interactive Berberine Derivatives. *Bioorg. Med. Chem. Lett. 16*, 1707–1711.

26. Cocco, M. J., Hanakahi, L. A., Huber, M. D., and Maizels, N. (2003) Specific Interactions of Distamycin with G-Quadruplex DNA. *Nucleic Acids Res. 31*, 2944–2951.

27. Martino, L., Virno, A., Pagano, B., Virgilio, A., Di Micco, S., Galeone, A., Giancola, C., Bifulco, G., Mayol, L., and Randazzo, A. (2007) Structural and Thermodynamic Studies of the Interaction of Distamycin A with the Parallel Quadruplex Structure [d(TGGGGT)]4. *J. Am. Chem. Soc. 129*, 16048–16056.

28. Maiti, S., Chaudhury, N. K., and Chowdhury, S. (2003) Hoechst 33258 Binds to G-Quadruplex in the Promoter Region of Human c-Myc. *Biochem. Biophys. Res. Commun. 310*, 505–512.

29. Cosconati, S., Marinelli, L., Trotta, R., Virno, A., Mayol, L., Novellino, E., Olson, A. J., and Randazzo, A. (2009) Tandem Application of Virtual Screening and NMR Experiments in the Discovery of Brand New DNA Quadruplex Groove Binders. *J. Am. Chem. Soc. 131*, 16336–16337.

30. Arya, D. P. (2005) Aminoglycoside-Nucleic Acid Interactions: The Case for Neomycin. *Top. Curr. Chem. 253*, 149–178.

31. Willis, B., and Arya, D. P. (2006) Major Groove Recognition of DNA by Carbohydrates. *Curr. Org. Chem. 10*, 663–673.

32. Willis, B., and Arya, D. P. (2006) An Expanding View of Aminoglycoside-Nucleic Acid Recognition. *Adv. Carbohydr. Chem. Biochem. 60*, 251–302.

33. Xi, H., Gray, D., Kumar, S., and Arya, D. P. (2009) Molecular Recognition of Single-Stranded RNA: Neomycin Binding to Poly(A). *FEBS Lett. 583*, 2269–2275.

34. Arya, D. P., Coffee, R. L., Jr., Willis, B., and Abramovitch, A. I. (2001) Aminoglycoside-Nucleic Acid Interactions: Remarkable Stabilization of DNA and RNA Triple Helices by Neomycin. *J. Am. Chem. Soc. 123*, 5385–5395.

35. Arya, D. P., Xue, L., and Tennant, P. (2003) Combining the Best in Triplex Recognition: Synthesis and Nucleic Acid Binding of a BQQ-Neomycin Conjugate. *J. Am. Chem. Soc. 125*, 8070–8071.

36. Xue, L., Charles, I., and Arya, D. P. (2002) Pyrene-Neomycin Conjugate: Dual Recognition of a DNA Triple Helix. *Chem. Commun. 1*, 70–71.

37. Arya, D. P., Coffee, R. L., Jr., and Charles, I. (2001) Neomycin-Induced Hybrid Triplex Formation. *J. Am. Chem. Soc. 123*, 11093–11094.

38. Arya, D. P., and Coffee, R. L., Jr. (2000) DNA Triple Helix Stabilization by Aminoglycoside Antibiotics. *Bioorg. Med. Chem. Lett. 10*, 1897–1899.

39. Xue, L., Xi, H., Kumar, S., Gray, D., Davis, E., Hamilton, P., Skriba, M., and Arya, D. P. (2010) Probing the Recognition Surface of a DNA Triplex: Binding Studies with Intercalator-Neomycin Conjugates. *Biochemistry* (*New York*) *49*, 5540–5552.

40. Xi, H., and Arya, D. P. (2005) Recognition of Triple Helical Nucleic Acids by Aminoglycosides. *Curr. Med. Chem. Anticancer Agents 5*, 327–338.

41. Shaw, N. N., and Arya, D. P. (2008) Recognition of the Unique Structure of DNA:RNA Hybrids. *Biochimie 90*, 1026–1039.

42. Shaw, N. N., Xi, H., and Arya, D. P. (2008) Molecular Recognition of a DNA:RNA Hybrid: Sub-Nanomolar Binding by a Neomycin-Methidium Conjugate. *Bioorg. Med. Chem. Lett. 18*, 4142–4145.

43. Arya, D. P., Shaw, N., and Xi, H. (2007) Novel Targets for Aminoglycosides, in *Aminoglycoside Antibiotics: From Chemical Biology to Drug Discovery* (Arya, D. P., Ed.) pp 289−314, Wiley, New York.

44. Arya, D. P., Xue, L., and Willis, B. (2003) Aminoglycoside (Neomycin) Preference is for A-Form Nucleic Acids, Not just RNA: Results from a Competition Dialysis Study. *J. Am. Chem. Soc. 125*, 10148–10149.

45. Arya, D. P., and Willis, B. (2003) Reaching into the Major Groove of B-DNA: Synthesis and Nucleic Acid Binding of a Neomycin-Hoechst 33258 Conjugate. *J. Am. Chem. Soc. 125*, 12398–12399.

46. Willis, B., and Arya, D. P. (2006) Recognition of B-DNA by Neomycin-Hoechst 33258 Conjugates. *Biochemistry* (*New York*) *45*, 10217–10232.

47. Willis, B., and Arya, D. P. (2009) Triple Recognition of B-DNA. *Bioorg. Med. Chem. Lett. 19*, 4974–4979.

48. Willis, B., and Arya, D. P. (2010) Triple Recognition of B-DNA by a Neomycin-Hoechst 33258-Pyrene Conjugate. *Biochemistry 49*, 452–469.

49. Arya, D. P., Coffee, R. L., Jr., and Xue, L. (2004) From Triplex to B-Form Duplex Stabilization: Reversal of Target Selectivity by Aminoglycoside Dimers. *Bioorg. Med. Chem. Lett. 14*, 4643–4646.

50. Napoli, S., Carbone, G. M., Catapano, C. V., Shaw, N., and Arya, D. P. (2005) Neomycin Improves Cationic Lipid-Mediated Transfection of DNA in Human Cells. *Bioorg. Med. Chem. Lett. 15*, 3467–3469.

51. Charles, I., Xi, H., and Arya, D. P. (2007) Sequence-Specific Targeting of RNA with an Oligonucleotide-Neomycin Conjugate. *Bioconjugate Chem. 18*, 160–169.

52. Charles, I., and Arya, D. P. (2005) Synthesis of Neomycin-DNA/peptide Nucleic Acid Conjugates. *J. Carbohydr. Chem. 24*, 145–160.

53. Charles, I., Xue, L., and Arya, D. P. (2002) Synthesis of Aminoglycoside-DNA Conjugates. *Bioorg. Med. Chem. Lett. 12*, 1259–1262.

54. Smith, F. W., and Feigon, J. (1992) Quadruplex Structure of Oxytricha Telomeric DNA Oligonucleotides. *Nature 356*, 164–168.

55. Haider, S. M., Parkinson, G. N., and Neidle, S. (2003) Structure of a G-quadruplex -Ligand Complex. *J. Mol. Biol. 326*, 117–125.

56. Campbell, N. H., Patel, M., Tofa, A. B., Ghosh, R., Parkinson, G. N., and Neidle, S. (2009) Selectivity in Ligand Recognition of G-Quadruplex Loops. *Biochemistry 48*, 1675–1680.

57. Piotto, M., Saudek, V., and Sklenar, V. (1992) Gradient-Tailored Excitation for Single-Quantum NMR Spectroscopy of Aqueous Solutions. *J. Biomol. NMR 2*, 661–665.

58. Goddard, T. D., and Kneller, D. G. SPARKY 3, University of California, San Francisco.

59. Smith, F. W., and Feigon, J. (1993) Strand Orientation in the DNA Quadruplex Formed from the Oxytricha Telomere Repeat Oligonucleotide d(G4T4G4) in Solution. *Biochemistry (New York) 32*, 8682–8692.

60. Schultze, P., Hud, N., Smith, F., and Feigon, J. (1999) The Effect of Sodium, Potassium and Ammonium Ions on the Conformation of the Dimeric Quadruplex Formed by the Oxytricha Nova Telomere Repeat Oligonucleotide d(G(4)T(4)G(4)). *Nucleic Acids Res. 27*, 3018–3028.

61. Trott, O., and Olson, A. J. (2010) AutoDock Vina: Improving the Speed and Accuracy of Docking with a New Scoring Function, Efficient Optimization, and Multithreading. *J. Comput. Chem. 31*, 455–461.

62. Schultze, P., Smith, F. W., and Feigon, J. (1994) Refined Solution Structure of the Dimeric Quadruplex Formed from the Oxytricha Telomeric Oligonucleotide d(GGGGTTTTGGGG). *Structure 2*, 221–233.

63. Pedretti, A., Villa, L., and Vistoli, G. (2004) VEGA—an Open Platform to Develop Chemo-Bio-Informatics Applications, using Plug-in Architecture and Script Programming. *J. Comput.-Aided Mol. Des. 18*, 167–173.

64. Sanner, M. F. (1999) Python: A Programming Language for Software Integration and Development. *J. Mol. Graphics Model. 17*, 57–61.

65. Arya, D. P., Micovic, L., Charles, I., Coffee, R. L., Jr., Willis, B., and Xue, L. (2003) Neomycin Binding to Watson-Hoogsteen (W-H) DNA Triplex Groove: A Model. *J. Am. Chem. Soc. 125*, 3733–3744.

66. Dominick, P. K., Keppler, B. R., Legassie, J. D., Moon, I. K., and Jarstfer, M. B. (2004) Nucleic Acid-Binding Ligands Identify New Mechanisms to Inhibit Telomerase. *Bioorg. Med. Chem. Lett. 14*, 3467–3471.

67. Buurma, N. J., and Haq, I. (2007) Advances in the Analysis of Isothermal Titration Calorimetry Data for Ligand-DNA Interactions. *Methods (Oxford, U.K.) 42*, 162–172.

68. Haq, I., Jenkins, T. C., Chowdhry, B. Z., Ren, J., and Chaires, J. B. (2000) Parsing Free Energies of Drug-DNA Interactions. *Methods Enzymol. 323*, 373–405.

69. Haq, I., Trent, J. O., Chowdhry, B. Z., and Jenkins, T. C. (1999) Intercalative G-Tetraplex Stabilization of Telomeric DNA by a Cationic Porphyrin. *J. Am. Chem. Soc. 121*, 1768–1779.

70. Record, M. T. J., Anderson, C. F., and Lohman, T. M. (1978) Thermodynamic Analysis of Ion Effects on the Binding and Conformational Equilibria of Proteins and Nucleic Acids: The Roles of Ion Association Or Release, Screening, and Ion Effects on Water Activity. *Q. Rev. Biophys. 2*, 103–178.

71. Jin, E., Katritch, V., Olson, W. K., Kharatisvili, M., Abagyan, R., and Pilch, D. S. (2000) Aminoglycoside Binding in the Major Groove of Duplex RNA: The Thermodynamic and Electrostatic Forces that Govern Recognition. *J. Mol. Biol. 298*, 95–110.

72. Xi, H., Kumar, S., Dosen-Micovic, L., and Arya, D. P. (2010) Calorimetric and Spectroscopic Studies of Aminoglycoside Binding to AT-Rich DNA Triple Helices. *Biochimie 92*, 514–529.

73. Kaul, M., and Pilch, D. S. (2002) Thermodynamics of Aminoglycoside-rRNA Recognition: The Binding of Neomycin-Class Aminoglycosides to the A Site of 16S rRNA. *Biochemistry (New York) 41*, 7695–7706.

74. Haider, S., Parkinson, G. N., and Neidle, S. (2002) Crystal Structure of the Potassium Form of an Oxytricha Nova G-Quadruplex. *J. Mol. Biol. 320*, 189–200.

75. Boger, D. L., Fink, B. E., Brunette, S. R., Tse, W. C., and Hedrick, M. P. (2001) A Simple, High-Resolution Method for Establishing DNA Binding Affinity and Sequence Selectivity. *J. Am. Chem. Soc. 123*, 5878–5891.

76. Tse, W. C., and Boger, D. L. (2004) A Fluorescent Intercalator Displacement Assay for Establishing DNA Binding Selectivity and Affinity. *Acc. Chem. Res. 37*, 61–69.

77. Allain, C., Monchaud, D., and Teulade-Fichou, M. P. (2006) FRET Templated by G-Quadruplex DNA: A Specific Ternary Interaction using an Original Pair of Donor/Acceptor Partners. *J. Am. Chem. Soc. 128*, 11890–11893.

78. Monchaud, D., Allain, C., and Teulade-Fichou, M. P. (2006) Development of a Fluorescent Intercalator Displacement Assay (G4-FID) for Establishing Quadruplex-DNA Affinity and Selectivity of Putative Ligands. *Bioorg. Med. Chem. Lett. 16*, 4842–4845.

79. Balagurumoorthy, P., Brahmachari, S. K., Mohanty, D., Bansal, M., and Sasisekharan, V. (1992) Hairpin and Parallel Quartet Structures for Telomeric Sequences. *Nucleic Acids Res. 20*, 4061–4067.

80. Mergny, J. L., and Lacroix, L. (2003) Analysis of Thermal Melting Curves. *Oligonucleotides 13*, 515–537.

81. Bishop, G. R., Ren, J., Polander, B. C., Jeanfreau, B. D., Trent, J. O., and Chaires, J. B. (2007) Energetic Basis of Molecular Recognition in a DNA Aptamer. *Biophys. Chem. 126*, 165–175.

82. Warui, D. M., and Baranger, A. M. (2009) Identification of Specific Small Molecule Ligands for Stem Loop 3 Ribonucleic Acid of the Packaging Signal Ψ of Human Immunodeficiency Virus-1. *J. Med. Chem. 52*, 5462–5473.

83. Holt, P. A., Chaires, J. B., and Trent, J. O. (2008) Molecular Docking of Intercalators and Groove-Binders to Nucleic Acids using Autodock and Surflex. *J. Chem. Inf. Model. 48*, 1602–1615.

84. Tan, J., Ou, T., Hou, J., Lu, Y., Huang, S., Luo, H., Wu, J., Huang, Z., Wong, K., and Gu, L. (2009) Isaindigotone Derivatives: A New Class of Highly Selective Ligands for Telomeric G-Quadruplex DNA. *J. Med. Chem. 52*, 2825–2835.

85. Ma, Y., Ou, T., Hou, J., Lu, Y., Tan, J., Gu, L., and Huang, Z. (2008) 9-N-Substituted Berberine Derivatives: Stabilization of G-Quadruplex DNA and Down-Regulation of Oncogene c-Myc. *Bioorg. Med. Chem. 16*, 7582–7591.

86. Wang, Y., and Patel, D. J. (1993) Solution Structure of the Human Telomeric Repeat d[AG₃(T₂AG₃)₃] G-Tetraplex. *Structure 1*, 263–282.